

FATIGUE CRACK GROWTH AND RESIDUAL STRENGTH OF CURVED FUSELAGE PANELS WITH MULTIPLE CRACKING

John G. Bakuckas, Jr., Lynn Pham, Catherine A. Bigelow, and Paul W. Tan

AAR-430

Airworthiness Assurance Research and Development Branch
FAA William J. Hughes Technical Center
Atlantic City International Airport, NJ 08405, USA

ABSTRACT

The effects of multiple cracks on the fatigue crack growth and residual strength of curved fuselage panels were studied in this research. A total of four panels were tested, two panels with a longitudinal lap splice and two with a circumferential butt joint. For each joint configuration, one panel contained only a lead crack and the other contained a lead crack with multiple cracks located along the outer critical rivet row of the joints. The Full-Scale Aircraft Structural Test Evaluation and Research (FASTER) facility was used for testing of the four curved panels. Geometric nonlinear finite element analyses were conducted to support the tests. The strain distributions and fracture parameters governing crack formation and growth were determined. Comparisons with strain gage data verified the finite element models. Results include comparisons of strain distributions, fatigue crack growth characteristics, and the damage growth process during residual strength test for the two joint configurations. In general, results reveal that multiple cracking did not have an effect on the overall global strain response. However, the number of cycles to grow a fatigue crack to a predetermined length was reduced by 37% and 27% for the longitudinal lap joint and circumferential butt joint panels, respectively by the presence of multiple-site cracking. In addition, the presence of multiple cracks reduced the residual strength of the panels with a longitudinal lap joint by approximately 20%.

INTRODUCTION

In order to assess the structural integrity of fuselage structure with multiple-site cracking scenarios and other problems associated with aging aircraft, a unique state-of-the-art facility was established at the Federal Aviation Administration (FAA) William J. Hughes Technical Center. The Full-Scale Aircraft Structural Test Evaluation and Research (FASTER) facility is capable of testing full-scale fuselage panel specimens under conditions representative of those seen by an aircraft in actual operation. The facility is designed to simulate the actual loads an aircraft fuselage structure is subjected to while in flight. Both quasi-static and spectrum loadings can be applied in the FASTER facility including differential pressure, longitudinal load, hoop load in the skin and frames, and shear load. A key component of the FASTER facility is the Remote-Controlled Crack Monitoring (RCCM) system, developed to track and record the formation and growth of multiple cracks in real-time during a test. Photographs of the FASTER facility and the RCCM are shown in Figure 1.

A complete description of the FASTER facility is provided in references 1 to 4. The system was designed using commercial-off-the-shelf (COTS) components whenever possible and to operate in an environment requiring minimal infrastructure support. The system was designed with safety considerations in mind by using water as the loading media. Using a simple

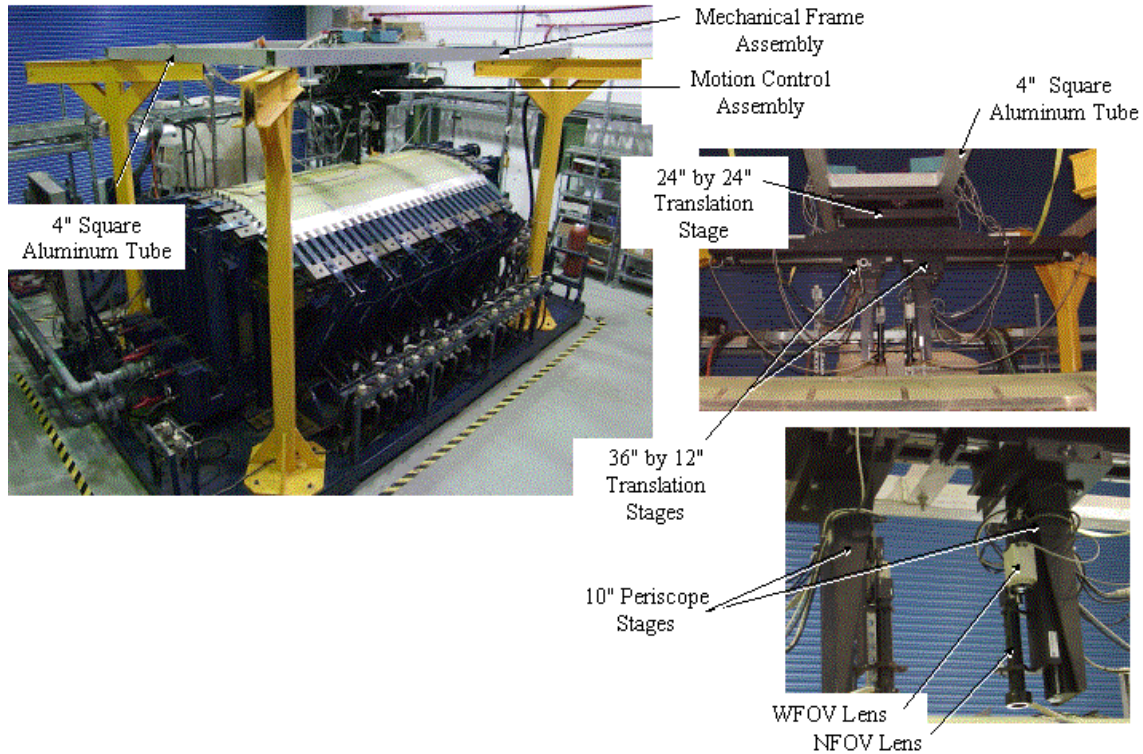


Figure 1. Photographs of FASTER facility and RCCM system

loading mechanism consisting of levers, fulcrums, and water actuators, complex mechanical loading is economically introduced. This simplified mechanical design concept in conjunction with a computer control and data acquisition system, presents a test system that is user friendly, has low cost of maintenance, is inherently safe, and is highly versatile.

The current test program is part of an effort to determine the effects of multiple cracking on the fatigue crack growth residual strength of curved fuselage structures. The curved panels used in the test program are similar to typical narrow-body fuselage structures consisting of skin, frames, shear clips, stringers, and either longitudinal splice or circumferential joints. A total of four panels were tested, two panels with a longitudinal lap splice and two with a circumferential butt joint. For each joint configuration, one panel (baseline) contained only a lead crack and the other contained a lead crack with multiple cracks.

Results for the baseline panels containing only a lead crack were reported in reference 4 for each joint configuration. For the baseline panels, strain survey was first conducted to ensure proper load introduction from the load application points. Fatigue crack formation and growth under constant amplitude cyclic loading were then monitored and recorded in real time using the RCCM system. After a prescribed amount of fatigue crack growth, each panel was loaded quasi-statically until failure and the crack extension and the residual strength were measured. Geometric nonlinear finite element analyses were conducted to obtain the fracture parameters governing crack formation and growth.

In this paper, experimental and analytical results for the companion panels containing multiple crack will be presented. The effects of the multiple cracks on the strain distributions, fatigue crack growth, and residual strength will be examined. In general, results reveal that multiple cracking did not have an effect on the overall global strain response. For fatigue crack growth in the baseline panels, when the lead crack grew into a neighboring rivet, a number of

cycles were required to reform the crack on the opposite side of the rivet (incubation period). For panels with multiple cracks, there was obviously no delay period needed since there were small cracks already at the rivets ahead of the lead crack. Hence, the number of cycles to grow the initial lead crack to a predetermined final length was reduced due to the presence of the small multiple cracks. Also, the multiple cracking reduced the residual strength of the fuselage panels tested. Analytical predictions agreed well with the test data.

EXPERIMENTAL PROCEDURE

Four panels were tested in this study: (1) panel CVP1 contains a longitudinal lap splice with a lead crack; (2) panel CVP2 has the same configuration and lead crack as CVP1 with the addition of multiple, small cracks emanating from rivet holes ahead of the lead crack; (3) panel CVP3 has a circumferential butt joint with a lead crack; and (4) panel CVP4 has the same configuration and lead crack as panel CVP3, with the addition of multiple, small cracks emanating from rivet holes ahead of the lead crack. These panels were subjected to a sequence of three loading functions: (1) initial monotonic quasi-static loading to a predetermined load level; (2) a constant amplitude cyclic loading; and (3) a postfatigue monotonic, quasi-static loading up to fracture.

Panel Configurations

The panel dimensions are 120" in the longitudinal direction, 68" in the circumferential direction, with a radius of 66" as shown for CVP1 and CVP2 in Figure 2. The panels tested represent narrow-body fuselage structure with either a longitudinal lap splice or a circumferential

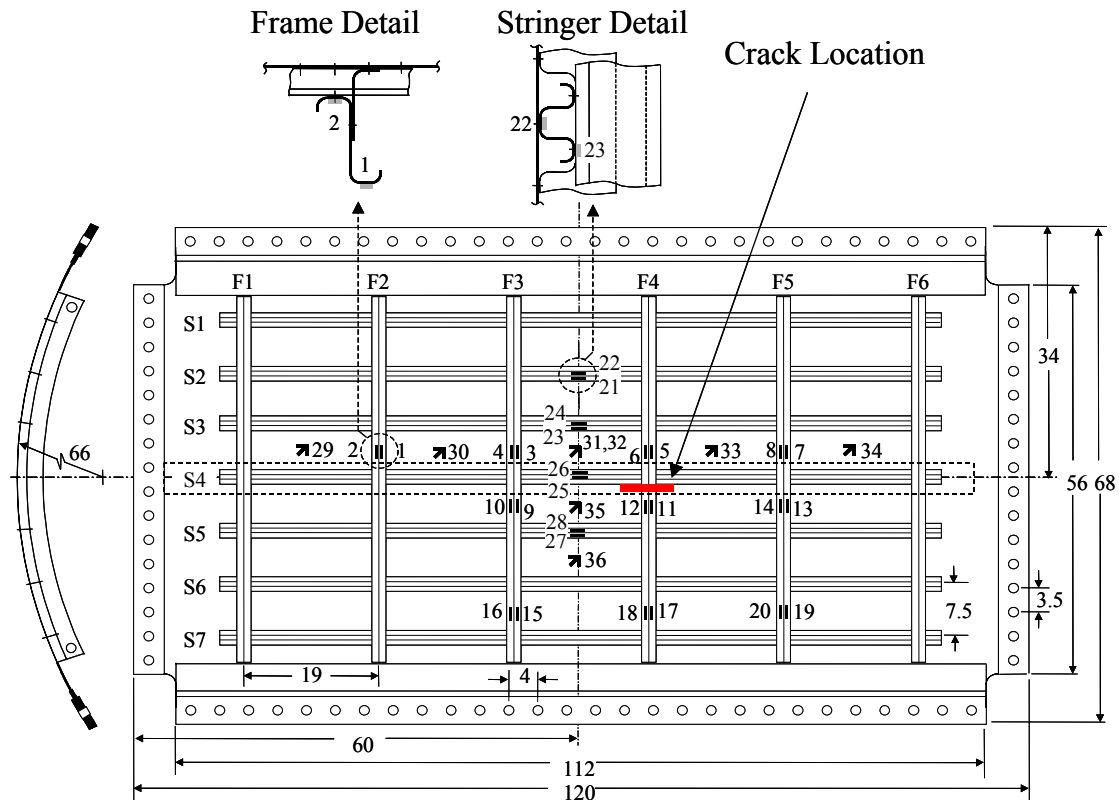


Figure 2. CVP1 and CVP2 panel configuration and strain gage locations

butt joint. The panel size was selected so that the test section could contain large damage such as a two bay crack with central frame severed. The test section of the panel was sized in order to minimize the effect of the test fixture attachment points along the perimeter.

Each panel had six frames with a 19" spacing and seven stringers with a 7.5" spacing. Z-shaped frames, L-shaped shear-clips, and hat-shaped stringers made from 7075-T6 aluminum were used. The edges of the panels, where loads are applied, were reinforced by bonding six layers of aluminum alloy doublers to the skin to ensure a uniform load transfer. Along the perimeter of the panel, reinforcing doublers with a length of 112" on the longitudinal sides and 56" on the hoop sides were added. All panels were instrumented with 64 strain gages in the skin, frames, and stringers.

A longitudinal lap joint was located along stringer S4, as shown in Figure 3, for the longitudinal lap joint panels CVP1 and CVP2. The joint consisted of two layers of the 2024-T3 panel skin with a thickness of 0.063" and two layers of 2024-T3 finger doublers with a thickness

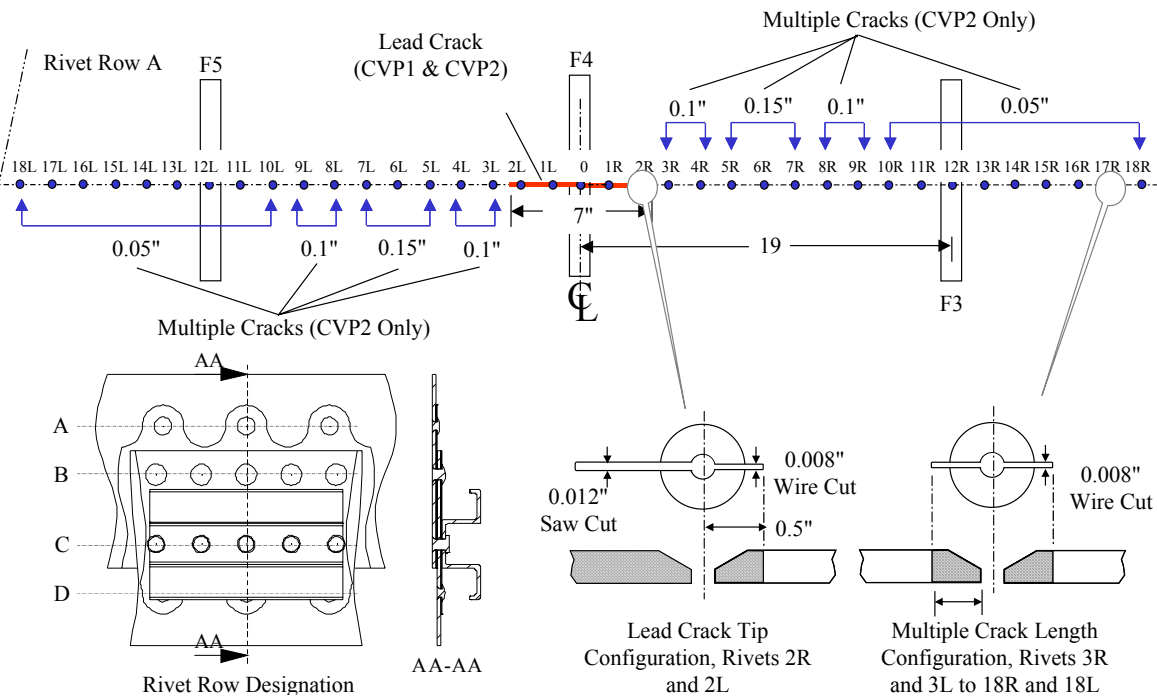


Figure 3. Joint configuration and initial damage for panels CVP1 and CVP2

of 0.025". Four rows of fasteners, A, B, C, and D were used to connect the skin and doublers. A crack-like slit representing a lead crack was placed symmetrically across frame F4, machined in the skin along the critical rivet row A in the longitudinal lap splice. The total length of the lead crack was 7.0". Between rivet holes 2L and 2R, the crack-like slit was saw cut with a width of 0.012". The tips of the lead crack, which emanated 0.5" from the centerline of rivet holes 2L and 2R, were wire cut with a width of 0.008". For panel CVP2, small multiple cracks were machined in the first 18 rivets to the left and right of the lead crack centerline rivet designated 0 with a width of 0.008". The nominal length of each crack is indicated in Figure 3.

For panels CVP3 and CVP4, a circumferential butt joint was located between frames F3 and F4 as shown in Figure 4. The joint consisted of two layers of the 2024-T3 panel skin with a thickness of 0.063", a 2024-T3 finger doubler with a thickness of 0.025", and a tapered doubler

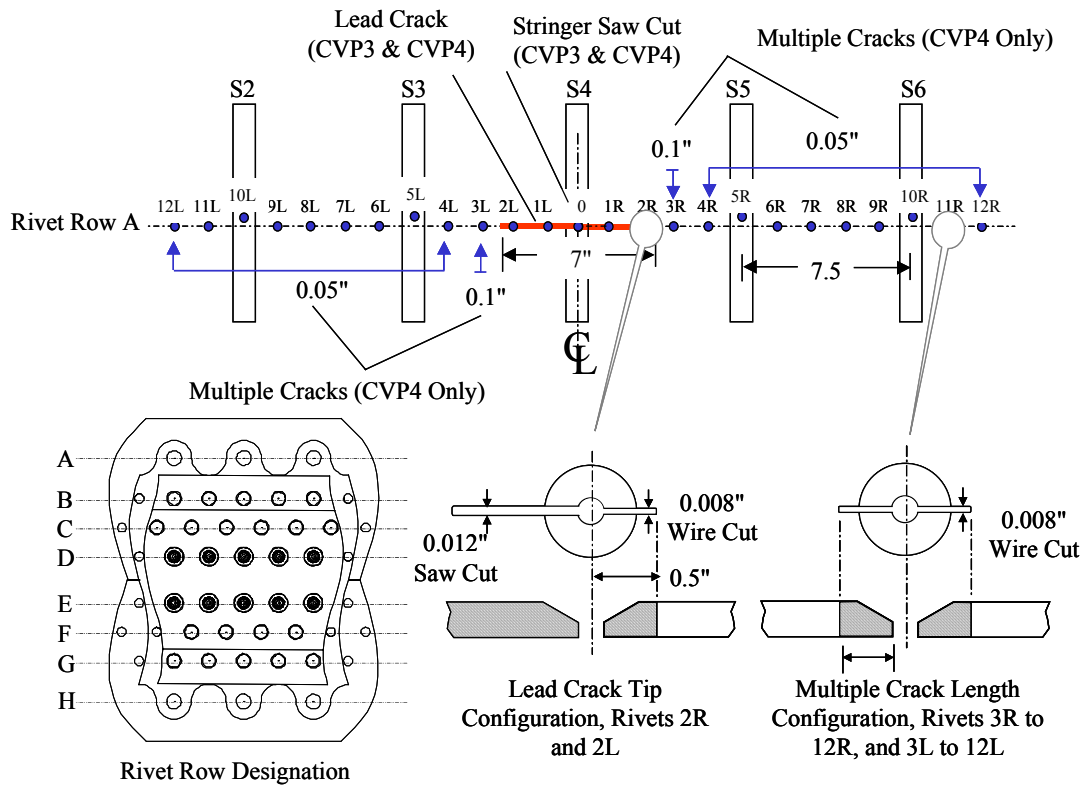


Figure 4. Joint configuration and initial damage for panels CVP3 and CVP4

with a maximum thickness of 0.071" which tapered to a thickness of 0.025" along edge. Eight rows of fasteners, A through H, were used to connect the skin and doublers. A crack-like slit representing a lead crack was placed symmetrically across stringer S4, machined in the skin along the critical rivet row A in the circumferential butt joint. Stringer S4 was cut to simulate a broken stringer. The total length of the lead crack was 7.0". Between rivet holes 2L and 2R, the crack-like slit was saw cut with a width of 0.012". The tips of the lead crack, which emanated 0.5" from the centerline of rivet holes 2L and 2R, were wire cut with a width of 0.008". For panel CVP4, small multiple cracks were machined in the first 12 rivets to the left and right of the lead crack centerline rivet designated 0 with a width of 0.008". The nominal length of each crack is indicated in Figure 4.

Test Conditions

The panels were subjected to the applied loadings listed in Table 1 for the strain survey, fatigue crack growth, and residual strength tests. For the longitudinal lap joint panels, the applied load simulates the cylindrical pressurization that a section of the fuselage along the neutral axis would experience. For the circumferential butt joint panels, the applied load

Table 1. Applied Loads

Panel	Maximum Load			
	Pressure (psi)	Hoop (lb/in)	Frame (lb/in)	Long. (lb/in)
CVP1	10.1	554.6	111.9	333.3
CVP2	10.1	554.6	111.9	333.3
CVP3	8.8	483.2	97.6	875.7
CVP4	8.8	483.2	97.6	875.7

simulates a fuselage down-bending condition that a fuselage section along the crown of the aircraft would experience, where the longitudinal stress is 50% higher than the hoop stress.

Quasi-static loadings were applied in ten equal increments up to the maximum loads listed in Table 1 to assess the strain distribution and reproducibility of the strain data. For fatigue crack growth tests, constant amplitude loading was applied at a frequency of 0.2 Hz with an R-ratio (minimum to maximum load) of 0.1. Fatigue crack growth of the lead crack and small multiple cracks were continuously monitored and recorded using the RCCM system. For the residual strength tests, the load was applied quasi-statically up to catastrophic failure proportionally to the values listed in Table 1.

Verification Testing

To verify test results generated using the FASTER facility, comparisons were made with results from a full-scale test conducted on an aft fuselage section of an actual narrow-body aircraft. The test article was pressurized quasi-statically from 0 to 7.8 psi for three tests. A section of aircraft, which closely resembles the curved panels tested, was instrumented with strain gages at the skin mid-bay, frame inner and outer caps, and the stringer cap and flange. Strains measured at these locations were compared with the strains measured at similar locations in longitudinal lap joint panels, CVP1 and CVP2, since the applied loading to this panel simulates the cylindrical pressurization of the aircraft.

ANALYSIS

Geometric nonlinear finite element analyses were conducted for each panel to determine strain distributions and mixed mode stress-intensity factor (SIF) solutions using the Modified Crack Closure Integral (MCCI) method [5 and 6]. The panels were modeled using two-dimensional shell elements with each node having six degrees of freedom. Figure 5 shows a

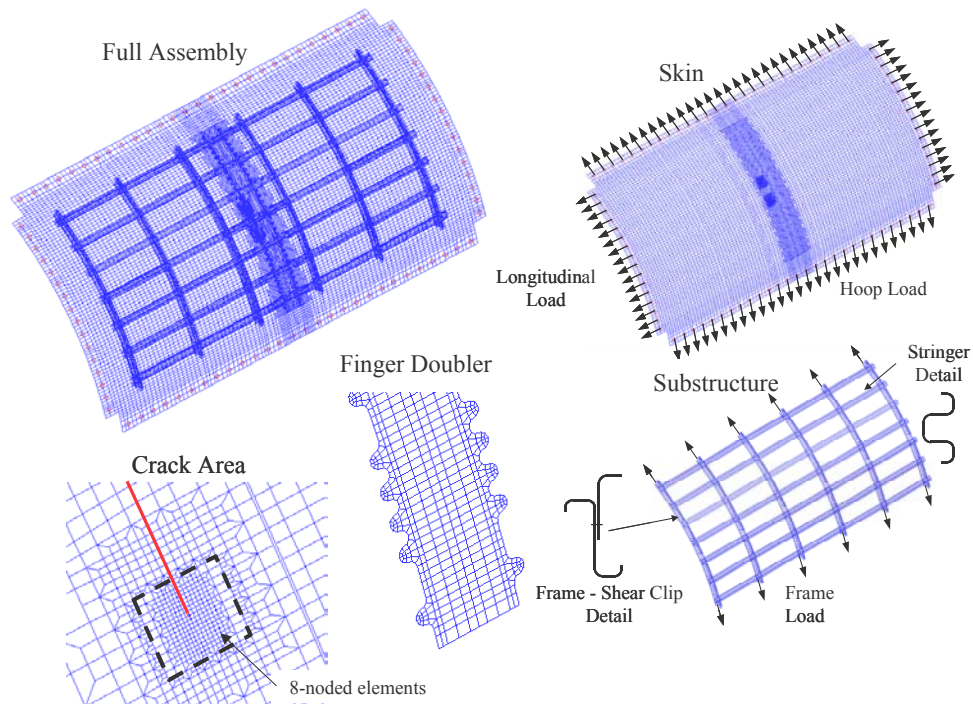


Figure 5. Finite element model of CVP3 showing full assembly and substructure components

global view of a typical finite element model of panel CVP3. A full description of the analysis conducted is provided in references 1 to 4. Four-noded shell elements were used throughout to model the skin, frames, shear clip, stringers, and intercostals except near the crack tips. In the immediate vicinity of the crack tips, eight-noded shell elements were used. The models contained the major geometric details of the panels including the cross-section properties of the substructure (frames, stringers shear-clip, intercostals), the dimensions of finger doublers, and the load attachment doublers. Beam elements were used to model the rivets that connected the substructures with the skin and the substructures to one another. Typically, the panel models had 250,000 degrees of freedom. The load conditions were simulated in the analysis. For the hoop, frame, and longitudinal loads, nodal point forces were applied at the load application points in the actual test as shown by the arrows in Figure 5. Internal pressure was applied to the inner surface of the skin.

RESULTS AND DISCUSSION

Representative results generated using the FASTER facility are presented in the following sections for the strain survey, fatigue crack growth, and residual strength testing.

Strain Survey

The strain distribution was measured and predicted under quasi-static load conditions listed in Table 1 for the panels tested. The hoop strain, as a function of applied pressure at a rosette strain gage, located in the skin mid-bay, is shown in Figure 6 for panel CVP1 (lead crack only) and panel CVP2 (lead crack and multiple cracks). The load was applied in ten equal increments up to the maximum values listed in Table 1.

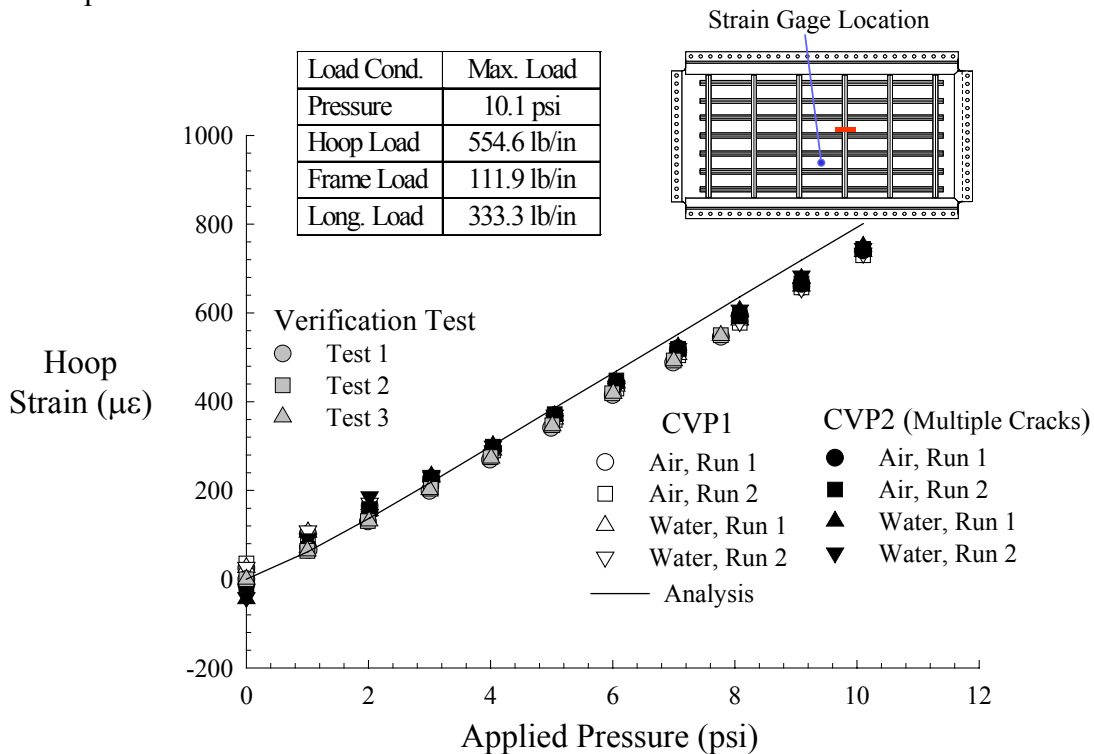


Figure 6. Hoop strain in gage located at skin mid-bay in panels CVP1 and CVP2 and verification full-scale test article

For each panel, the test was repeated twice using water and twice using air. As shown in the figure, the strains are nearly identical for both panels for all four runs indicating that small multiple cracks have no effect on the global strain response at the given load level. As expected, there were no differences in the results when air or water was used to pressurize the panel. In addition, the three sets of results from the full-scale verification test, measured from a rosette strain gage in the skin mid-bay location, are plotted in Figure 6. The verification full-scale test results are repeatable and closely follow the results from CVP1 and CVP2 panels up to the maximum pressure of 7.8 psi. This indicates that the applied loading closely resemble the pressurization of a fuselage structure. Also shown in Figure 6, is a plot of the result predicted using the finite element analysis as described previously. The prediction from analysis shown by the solid curve in the figure is in good agreement with the experimental data validating the finite element analysis.

In general, similar trends in strain gage data were obtained at the other gage locations in the panels tested. That is, experimental results were very repeatable and the analytical predictions were in good agreement with the test results. Measured strains were nearly uniform in the middle of the panel. This provides confidence that the applied loads were introduced properly and the models have enough fidelity to capture the mechanical response. In addition, the small multiple cracks had no effect the global strain response.

Fatigue Crack Growth

The fatigue crack growth was measured during the constant amplitude loading defined by loads in Table 1. Representative results are presented. Photographs of crack extension of the lead crack and the smaller multiple cracks under fatigue loading obtained from the RCCM system are shown in Figure 7 for panel CVP4. The photographs illustrate the damage growth from the original slit of the lead crack and the multiple-site cracks at the first adjacent rivets on either side (3R and 3L). The block size of the grid paper on the top of each photograph is 0.05".

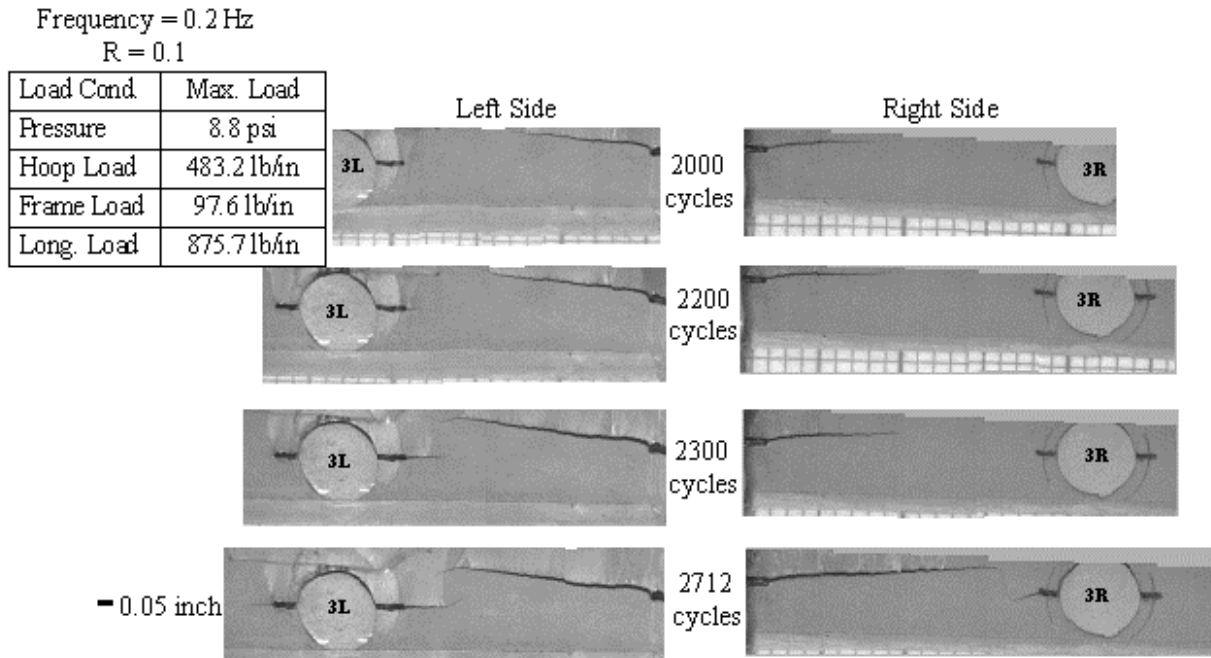


Figure 7. Photographs of crack growth in panel CVP4 using RCCM system

The fatigue crack growth behavior of panels CVP1 and CVP2 is shown in Figure 8. The initial half crack length prior to loading was approximately 3.5". In the figure, the circular and square symbols represent the measured crack lengths at both the left and the right crack tips, respectively, for each panel. The numbers inside the circles along the y axis represent the

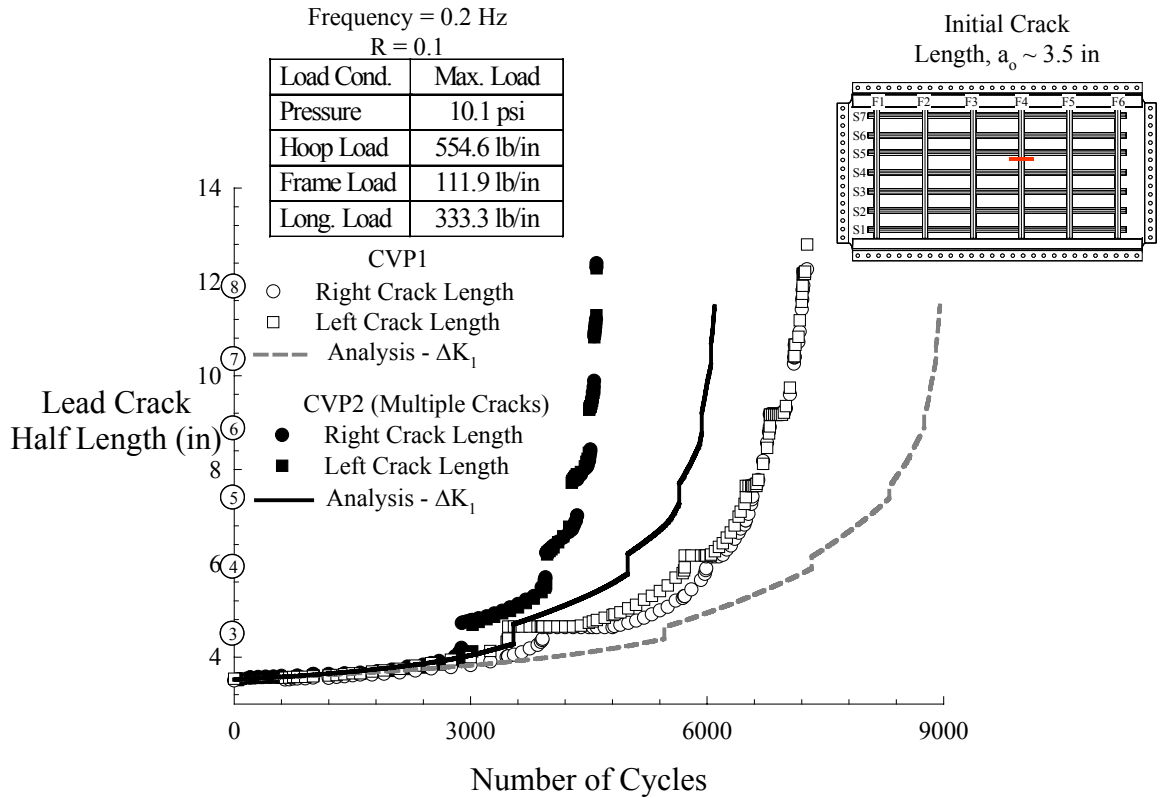


Figure 8. Half-length of the lead crack as a function of number of fatigue cycles for panels CVP1 and CVP2

location of rivets. For panel CVP1, shown with the open symbols, the vertical jumps indicate crack extension across a rivet hole. When this happened, the crack length increased instantaneously by the diameter of the rivet hole. The rate of crack growth increased as the crack tips approached the rivet holes. The horizontal segments shown in the plot indicate the number of cycles before the crack reformed on the opposite side of the rivet hole. As the crack length increased, the delay in crack reformation (incubation period) decreased due to the larger crack driving force. For panel CVP2, which contained multiple cracks, the vertical jumps in the experimental data indicate linkup of the lead crack and a small multiple crack. When this happened, the crack length increased instantaneously by the diameter of the rivet hole plus the lengths of the small cracks at that rivet. There was no crack reformation. The length of the lead crack front instantaneously grew the length of the small cracks located in the rivets directly ahead. As a result, the number of cycles needed to grow the lead crack to the final length (~12.5inches) in panel CVP2 was approximately 37% less than that in panel CVP1.

The Mode I stress-intensity factor range was used in a cycle-by-cycle crack growth analysis program to predict the fatigue crack growth in panels CVP1 and CVP2, also shown in Figure 8. The rivet holes were not explicitly modeled in the finite element analysis. For panel CVP1, crack growth across rivet holes, indicated by the vertical jumps in the curve, was modeled

by instantaneously increasing the length of the crack by the diameter of the rivet hole when the crack reached the rivet. For panel CVP2, crack growth across the rivets was modeled by instantaneously increasing the length of the crack by the diameter of the rivet plus the length of the small cracks at the rivet when the lead crack reached the first small multiple crack. Good agreement was obtained between experiments and predictions relying on the mode I stress-intensity factor range. For CVP2, the growth of the small multiple crack in the rivet ahead of the lead crack was not accounted for in the analysis.

Similar trends in the results were obtained for the circumferential butt joint panels, CVP3 and CVP4. In general, symmetric, collinear crack propagation was observed using the Remote Control Crack Monitoring (RCCM) system. Reasonable agreement was obtained between experimental fatigue crack growth data and predictions relying on the Mode I stress-intensity factor ranges calculated using finite element analyses of the test panels. The number of cycles to grow a fatigue crack to a predetermined length was reduced by approximately 27% due to the presence of multiple cracks for the circumferential butt joint panels.

Residual Strength

Residual strength of panels was measured under quasi-static loading conditions. Typical results from the residual strength test of panels CVP1 and CVP2 (contained multiple cracks) is shown in Figure 9 where the square and circular symbols represent the crack extension for the

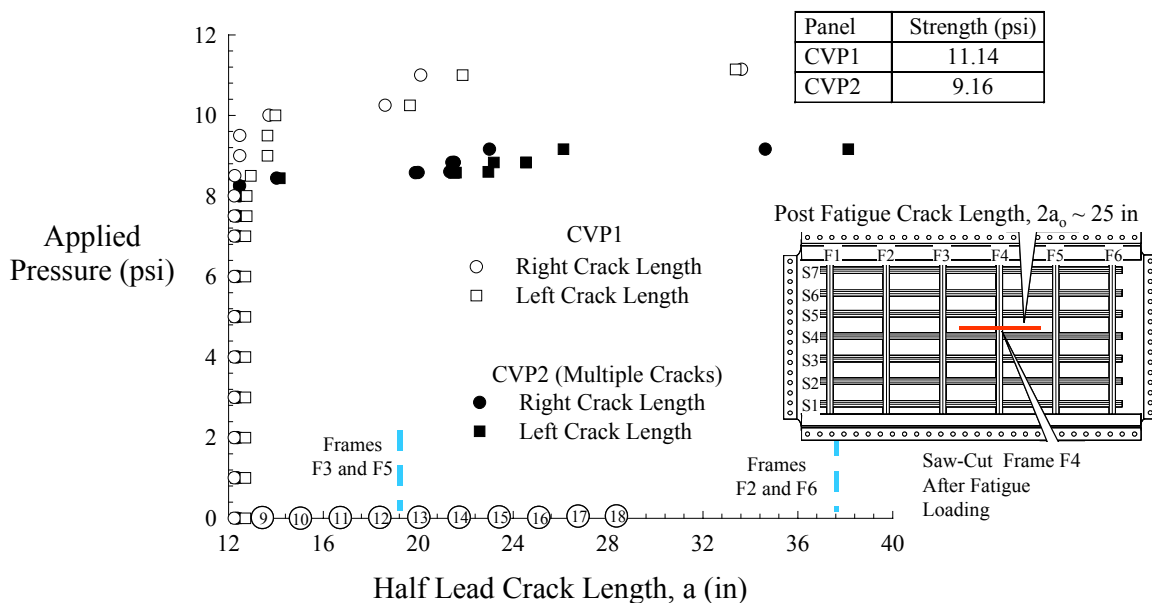


Figure 9. Crack extension during residual strength tests for panels CVP1 and CVP2

left and right crack tips, respectively. The numbers inside the circles along the x axis indicate the rivet location. During the test, cylindrical pressurization was applied quasi-statically, and the crack extension measured up to panel failure. In the initial stages of loading, slow stable crack extension was observed in both panels up to 10.25 psi pressure for panel CVP1 and 8.5 psi pressure for panel CVP2. Then, the crack grew rapidly through rivets 9 through 11 on both the right and left side to the first intact frames (F3 and F5) for both panels and then was arrested. An increase of pressure was required to grow the cracks past the frames in both panels, and stable crack extension continued until catastrophic failure occurred at 11.14 psi for panel CVP1 and

9.16 psi for panel CVP2. The presence of multiple cracks reduced the residual strength by approximately 20%.

During the residual strength test of panel CVP3, premature failures occurred at the load application points. As a consequence, the effect of multiple cracking on the residual strength of the circumferential butt joints cannot be accurately quantified since an accurate determination of the residual strength of panel CVP3 could not be made. However, the effect of multiple cracking on the damage growth process can be determined up to the point of the premature failure of CVP3. Figure 10 shows the results from the first residual strength test for panel CVP3 and the residual strength test for panel CVP4. In this figure, the numbers inside the circles along the x axis indicate the location of rivets. For panel CVP3, growth of the lead crack was slow and stable up to rivet 7. A continuous increase in load was required to extend the crack. However, the load attachment point failed prematurely. For panel CVP4, once the lead crack started to grow, the subsequent growth was very rapid through rivet 7. Catastrophic failure of panel CVP4 occurred at a pressure of 20.75 psi.

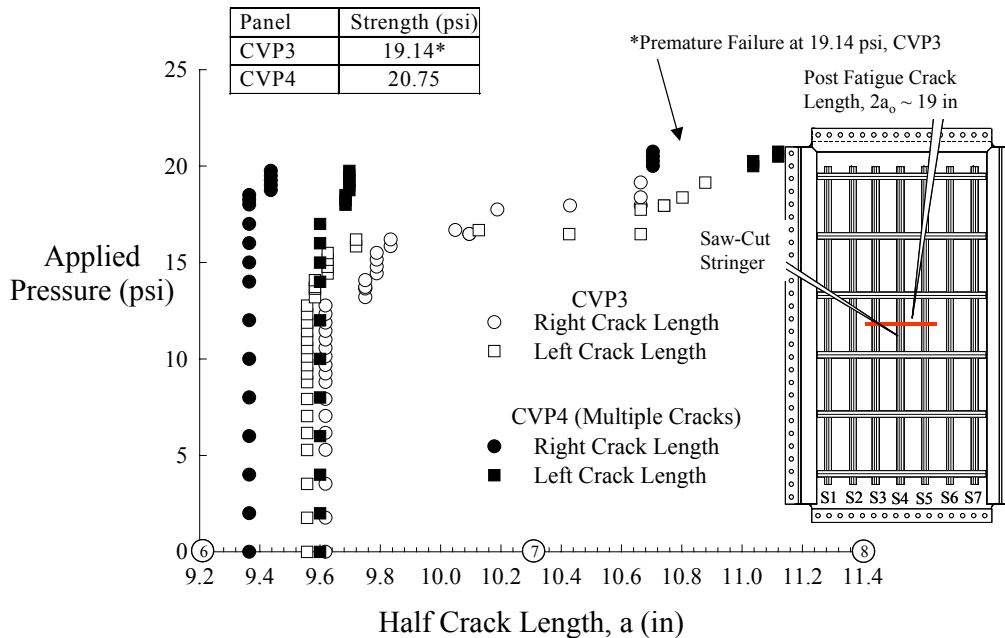


Figure 10. Crack extension, as a function of applied pressure, recorded for residual strength tests of panels CVP3 and CVP4

CONCLUDING REMARKS

An experimental and analytical investigation was undertaken to assess the effects of multiple-site cracking on the fatigue crack growth and residual strength characteristics of curved panels. The Full-Scale Aircraft Structural Test Evaluation and Research (FASTER) facility was used to apply realistic loading conditions to curved panels representing fuselage sections. Both quasi-static and constant amplitude fatigue loadings were applied to the panels. A geometrically nonlinear finite element analysis was used to determine the strain distribution in the panels and the fracture parameters necessary for predicting the fatigue crack growth behavior of the panel were calculated.

A total of four panels were tested, two panels with a longitudinal lap splice and two with a circumferential butt joint. For each joint configuration, one panel contained only a lead crack and the other contained a lead crack with small multiple cracks. Strains were measured under quasi-static loading conditions to ensure proper load introduction to the panels. The strain measurements were highly repeatable and were in good agreement with the finite element analyses. The presence of multiple cracks did not affect the overall global strain response. Symmetric, collinear crack propagation was observed under constant-amplitude fatigue loading using the Remote Control Crack Monitoring (RCCM) system. Reasonable agreement was obtained between experimental fatigue crack growth data and predictions relying on the Mode I stress-intensity factors calculated using finite element analyses of the test panels. The number of cycles to grow a fatigue crack to a predetermined length was reduced by approximately 37% due to the presence of multiple cracks for the longitudinal lap joint panels and 27% for the circumferential butt joint panels. Residual strength tests were conducted on each panel after the fatigue loading. For the curved panels with the longitudinal lap splice, the presence of multiple cracks reduced the residual strength by approximately 20%. For the curved panels with the circumferential butt joint, the residual strength of the baseline panel containing only a lead crack was not measured due to premature failures at the load application points. Consequently, the effect of multiple cracks on the residual strength of the circumferential butt joint configuration could not be quantified. However, it was observed that the growth of lead crack into the first rivet directly ahead was more rapid for the panel containing multiple cracks.

REFERENCES

1. Bakuckas, J. G. Jr., "Full-Scale Testing of Fuselage Structure Containing Multiple Cracks," DOT/FAA/AR-01/46, 2001.
2. Bakuckas, J. G., Jr., Bigelow, C. A., and Tan, P. W., "The FAA Full-Scale Aircraft Structural Test Evaluation and Research (FASTER) Facility," *Proceedings from the International Workshop on Technical Elements for Aviation Safety*, Tokyo, Japan, pp. 158-170, 1999.
3. Bakuckas, J. G., Jr., Akpan, E., Zhang, P., Bigelow, C. A., Tan, P. W., Awerbuch, J., Lau, A., and Tan, T. M., "Experimental and Analytical Assessments of Multiple-Site Cracking in Aircraft Fuselage Structure," *Proceedings of the 20th Symposium of the International Committee on Aeronautical Fatigue*, Seattle, Washington, USA, July 14-15, 1999.
4. Akpan, E., Zhang, P., Bakuckas, J. G., Jr., Tan, P. W., Awerbuch, J., Lau, A., and Tan, T. M., "Full-Scale Testing of Fuselage Structure with Cracks," *Proceedings of the 4th Joint DoD/FAA/NASA Conference on Aging Aircraft*, St. Louis, Missouri, USA, May 15-18, 2000.
5. Rybicki, E. F. and Kanninen, M. F., "A Finite Element Calculation of Stress-Intensity Factors by a Modified Crack Closure Integral," *Engineering Fracture Mechanics*, Vol. 9, pp. 931-938, 1977.
6. Viz, M. J., Potyondy, D. O., and Zehnder, A. T., "Computation of Membrane and Bending Stress-Intensity factors for Thin, Cracked Plates," *International Journal of Fracture*, Vol. 72, pp. 21-38, 1995.